A Method for Optimal GMTI Focussing and Enhanced Visual Evaluation

Michael, Eineder, DLR, Germany
Richard, Bamler, DLR, Germany
Steffen, Suchandt, DLR, Germany

Abstract

Ground moving target indication (GMTI) from spaceborne SAR data has been successfully demonstrated by the authors with data from the Shuttle Radar Topography Mission: signatures could be assigned to larger vehicles on highways and their velocity could be estimated. In consequence of these results, a number of systematic experiments were conducted with DLR's airborne SAR ESAR in preparation for the German satellite TerraSAR-X to be launched in 2006. Future SAR satellites like the TerraSAR-X and the Canadian Radarsat-2 will offer advanced imaging modes optimized for GMTI, e.g. using split antennas and dual or triple receive channels. Currently, an operational GMTI processing system is being developed at DLR in order to generate traffic information for civilian use from TerraSAR-X data. This paper proposes solutions for two problems occurring in such a processing and evaluation chain: Firstly, optimal SAR focussing of moving targets is not straightforward since the target motion changes the synthetic aperture parameters which have to be precisely adapted in the SAR processor. If not adapted, the target appears unfocussed and ambiguous. Secondly, moving objects appear displaced from the stationary clutter in the image making the evaluation by a human interpreter difficult. Both problems are solved simultaneously by a rigorous modelling of the imaging process and by incorporating a-priory knowledge in the processing and evaluation chain. The results will be optimally focussed GMTI images that can be easily evaluated by a human operator.

1. Introduction

Already before the launch of the Shuttle Radar Topography Mission (SRTM) [6] it was known that the 7 meter along track baseline component between primary and secondary antenna would allow measuring moving objects such as rivers and even road vehicles. Controlled experiments were conducted during the mission to investigate whether or not this effect could be used to measure the speed of cars [1]. Soon after the processing of SRTM data had commenced at DLR, spurious phase anomalies were found near some highways, which could only be caused by larger moving vehicles such as trucks [1]. All those results motivated us to closer investigate the capabilities of spaceborne SAR sensors for traffic monitoring [2], [3], [5]. The encouraging results of these studies led to the implementation of the Dual Receive Antenna (DRA) mode for the TerraSAR-X satellite [4] by electronically splitting the SAR antenna in flight direction into two halves and recording their signals separately using two parallel receive channels. The high resolution of TerraSAR-X, which is in the one meter range, also enables the detection of single vehicles. For the processing of the DRA mode data a moving target processing system is currently being developed at DLR in cooperation with the Technical University of Munich [8]. This paper discusses some novel focusing algorithms to correct for the distortion effects of moving objects.

2. Velocity Measurement with SAR

A SAR system exploits its own motion along a flight track to synthesize a large aperture and hence a high resolution in azimuth. As the flight track forms the aperture it must be known with very high precision. If the imaged object has an additional velocity component relative to the SAR, this causes a number of effects, which may either help or hinder the detection of a moving object and the estimation of its velocity. Firstly, objects with a *line-of-sight* (LOS) velocity component $\mathrm{v_r}$ appear displaced along the flight track in the image. This displacement is proportional to the vehicle's velocity component $\mathrm{v_r}$ and is given by

$$\Delta a = \frac{\mathrm{v_r}}{\mathrm{v_{SAR}}} R \,, \qquad (1)$$

where R is the distance between antenna and object, and v_{SAR} is the velocity of the SAR antenna. The LOS velocity component also introduces a shift Δf_{DC} of the object's Doppler spectrum relative to the Doppler spectrum of the stationary background. This shift is proportional to Δa :

$$\Delta f_{DC} = \frac{2\mathrm{v_{SAR}}\Delta a}{\lambda R} \,, \qquad (2)$$

where λ is the wavelength of the SAR.
Secondly, a motion component of the object *parallel* to the SAR antenna alters the relative velocity between object and sensor, which leads to defocusing.

Thirdly, due to the LOS motion of moving objects they appear slightly range displaced in the two acquisitions of the DRA mode data. A simple way to exploit this fact and to measure the object's velocity is to calculate the interferometric phase difference

$$\phi_{ATI} = \frac{2\pi}{\lambda} \mathrm{v_r} \cdot \frac{B_{ATI}}{\mathrm{v_{SAR}}} \qquad (3)$$

between the images derived from two antennas separated by B_{ATI} in flight direction.

In practice the detection of vehicles and the estimation of their velocities is difficult with spaceborne and airborne SARs, as their signal is rather low, defocused by their motion, superimposed on the background clutter and displaced far away from the road. In the following we propose algorithms to optimally process and visualize such data in order to simplify the detection of moving vehicles.

3. Focusing Moving Target Data

Conventional SAR processors for stationary targets use constant values for FM rate (for every range value) and Doppler centroid within azimuth blocks for efficient data processing. Since we need to update parameters from pixel to pixel in the scene in order to optimally focus moving vehicles, other solutions are required.

One brute-force solution would be, to process a stack of images using all relevant combinations of Doppler shift Δf_{DC} and frequency modulation rate shift ΔFM caused by the cross track velocity components $\mathrm{v_r}$ and the along track velocity component $\mathrm{v_a}$, respectively. Then, a final velocity adapted image would be composed by taking the correct $\Delta f_{DC}, \Delta FM$ combination for each pixel from the resulting stack that is expected from its distance to the road and the corresponding road angle. However, depending on the expected velocity range and the tolerable focusing error, this data stack might consist of hundreds of images. The enormous computational load and the postponed problem how to fuse and further process the data stack is a limitation to this approach.

4. Velocity Adapted Processing

The key idea of our approach is to use the three-dimensional knowledge of the road track for the focusing process. We only focus the relevant areas close to the road (the along-track displacement of moving objects is limited by the maximum speed) and adapt the focusing parameters according to the hypothetical velocities $\mathrm{v_r}$ and $\mathrm{v_a}$ that are unique to each pixel.

The processing sequence of the method is as follows:

1) Transformation of the road track coordinate samples {(x, y, z), …} into the SAR zero-Doppler azimuth / range image coordinate system {(a_S, r_S) …}

2) Interpolation of the road track so that it is known for each range pixel of the image.

3) The maximal target velocity $\mathrm{v_{max}}$ and the system's PRF define a maximal azimuth shift for each range position, which can be calculated by evaluating $\Delta a = \frac{\mathrm{v_{max}} \sin(\alpha)\sin(\theta)}{\mathrm{v_{SAR}}} R$. Thus, Δa depends on the incidence angle θ and the local angle α between road and flight track. The limitation of the search space to the azimuth area $\{[a_S-\Delta a_{max},\ a_S+\Delta a_{max}],\ r_S\}$ significantly reduces the load of further processing. Within this search space we determine the LOS vehicle velocity for each pixel from the azimuth distance between pixel and road under the hypothesis that this pixel contains a moving object:

$$\mathrm{v_r} = \frac{a - a_S}{\mathrm{v_{SAR}}} R\,. \qquad (4)$$

4) Projection of this pixel along azimuth on the road indicates the true position of the car. From the imaging geometry at this position and the heading of the road we can estimate the target's azimuth velocity component:

$$\mathrm{v_a} = \frac{\mathrm{v_r}}{\tan\alpha \cdot \sin\theta}\,. \qquad (5)$$

5) Knowing $\mathrm{v_a}$ and $\mathrm{v_r}$ we adjust the frequency modulation rate of the SAR processor for each pixel by ΔFM and the Doppler centroid by Δf_{DC}. Both corrections are computed using the precise imaging geometry as performed in modern SAR processors. The improvements reached by using an adaptive algorithm are shown in Fig. 1 and Fig. 2. Figure 1 shows a SAR scene processed with the standard SAR processor fed with stationary parameters while Fig. 2 shows SAR data processed with velocity adapted parameter update using the time domain algorithm described in section 4.1. Note the moving targets that appear much brighter than if processed with the standard SAR processor. This image must be interpreted as follows: Only objects on the road are focused correctly. Moving objects are displaced from the road depending on their range velocity. Stationary objects off the road are defocused. Ambiguity images appear further away from the road. Targets moving on the road are focused correctly, while the stationary road in the ambiguity image is focused with a Doppler centroid off by ± PRF and hence wrong range migration.

In the following we discuss several different implementation variants of such a velocity adapted focusing algorithm.

4.1. Time Domain Focusing

An elegant and mathematically correct implementation is a time domain algorithm which is optimal in terms of image quality. In a first step, this approach performs a range compression of the raw data using fast convolution. The azimuth compression is then performed in time domain by back projection of the focused image sample into the raw data while considering its hypothetic motion at the same time. Figure 2 shows the result of a time domain back projection focusing of SRTM X-SAR data. As the azimuth aperture is only of about 300 samples length, the correlation can be conveniently performed in time domain. SAR systems with longer aperture such as C-band or L-band sensors may render the time domain method impracticable. Therefore, more efficient algorithms are proposed in the following.

4.2. Controlled Stack Processing

In this variant we propose to use a modified SAR processor, e.g. a chirp scaling processor to process a data stack with varying parameters. Compared to pure parallel processing the efficiency is significantly increased by the following steps:

1) generate a control mask containing the corrective focusing parameters for each pixel and a flag for irrelevant pixels, i.e. if the velocities are not reasonable

2) quantize the corrective parameters Δf_{DC} in N, and the ΔFM parameters in M steps

3) perform all range pre-processing steps and the range compression for the whole SAR image (for the TerraSAR-X processor this is about 60 % of the total processing effort)

4) perform azimuth compression for all $\Delta f_{DC}, \Delta FM$ parameters of the matrix resulting in N x M images (for one image this is about 40 % of the effort)

5) compose one image from the N x M images by selecting each pixel from the layer where the $\Delta f_{DC}, \Delta FM$ parameters match the range and azimuth velocities as described in section 4

The result is an image comparable to the time domain approach, but with quantized approximations of the focusing parameters.

4.3. Azimuth Spectrum Replication and Velocity Adapted Filtering

For TerraSAR-X we can assume that the velocity induced Doppler shifts are within two PRF bands and the defocusing due to along-track velocities is small, i.e. in the order of 10 pixels. Due to these facts we can find a compact, and currently preferred processing variant with time domain post processing:

1) use a slightly modified SAR processor that replicates the Doppler (azimuth) spectrum after range compression such that the entire range of expected Doppler frequencies is covered. This can be any non-integer multiple of the PRF. In consequence, ambiguity images are produced and appear overlaid in the raw image. The range migration for the ambiguity images is correctly applied in the processor. The result is one conventional single look complex image.

2) perform a time domain post band-pass filtering and post residual focusing of the azimuth spectrum with the space variant parameters $\Delta f_{DC}, \Delta FM$ as derived in section 4. This way the ambiguity images are removed and the defocusing is corrected.

The result is again a velocity adapted image which is well suited as an input for ATI or DPCA detectors.

5. Visualization Enhancements

The visual interpretation of such velocity adapted images is simplified by projecting iso-velocity contour lines along the road, in analogy with contour lines on topographic maps. They are easily derived following the equations in section 4. Using the iso-velocity contours, a trained operator can identify single cars or chains of cars in the image. He additionally can quickly assess the plausibility of the velocity by visually interpolating the position between contour lines.

In the case of along-track interferometry both the phase of moving cars and the iso-velocity contours can additionally be color coded with the measured and expected phase, respectively. This additional information allows to solve PRF and phase ambiguities if their corresponding velocities are different.

6. Simplifications Made

We assumed only one dominant road in our image. As mentioned in [8], the assignment of a pixel to its corresponding road may no longer be straightforward in urbanized areas with dense road networks. In this case the described velocity adapted processing must be performed for each road relevant for this pixel.

The estimation of the range velocity from the azimuth displacement and the derivation of the azimuth velocity from the road angle fail for flight tracks which are almost parallel to the road. In this case the azimuth velocity can be estimated by autofocus algorithms as described in [3].

Range accelerations lead to defocusing effects comparable to and indistinguishable from effects caused by azimuth velocities [7]. However, acceleration effects caused by curved roads can be estimated and compensated for within the presented approach without increasing the numerical complexity, if a constant target velocity can be assumed.

7. Future Work

Up to now prototypes and demonstrators have been implemented and tested with SRTM and airborne E-SAR data. The selection of the final algorithm has yet to be done and will be based on an analysis of the processing speed and quality of the respective variants using true TerraSAR-X imaging parameters.

8. References

[1] Breit, H.; Eineder, M.; Holzner, J.; Runge, H.; Bamler, R.: Traffic Monitoring using SRTM Along-Track Interferometry, Proc. of IEEE IGARSS'03, Toulouse, 2003.

[2] Meyer, F., Hinz, S.: The Feasibility of Traffic Monitoring with TerraSAR-X - Analyses and Consequences, Proc. of IEEE IGARSS 2004, Anchorage, 2004.

[3] Meyer, F., Hinz, S., Laika, A., Bamler, R.: A-priori Information Driven detection of Moving Objects for Traffic Monitoring by SAR. Proc. of IEEE IGARSS'05, Seoul, South Korea, 2005.

[4] Mittermayer, J.; Runge, H.: Conceptual Studies for Exploiting the TerraSAR-X Dual Receive Antenna, Proc of IEEE IGARSS 03, Toulouse/France, 2003.

[5] Palubinskas, G.; Runge, H.; Reinartz, P.: Radar signatures of road vehicles, Proc. of IEEE International Geoscience and Remote Sensing Symposium, IGARSS 04, Anchorage, pp. 1498-1501, 2004.

[6] Rabus, B., Eineder, M., Roth, A., Bamler, R., The Shuttle Radar Topography Mission (SRTM) – A New Class of Digital Elevation Models Acquired by Spaceborne Radar, ISPRS Journal of Photogrammetry & Remote Sensing, 57, pp. 241-262, 2003.

[7] Sharma, J.J., Gierull, C.H., Collins, M.J.: The Influence of Target Acceleration on Velocity Estimation in Dual Channel SAR-GMTI, IEEE Trans. Geosc. And Remote Sensing, vol. 44, no.1, January 2006, pp. 134-147.

[8] Suchandt, S., Eineder, M., Müller, R., Breit, H., Reinartz, P., Laika, A., Meyer, F., Palubinskas G. and Runge, H., A GMTI Processing System for the Extraction of Traffic Information from TerraSAR-X Data, EUSAR 2006, Dresden, 2006.

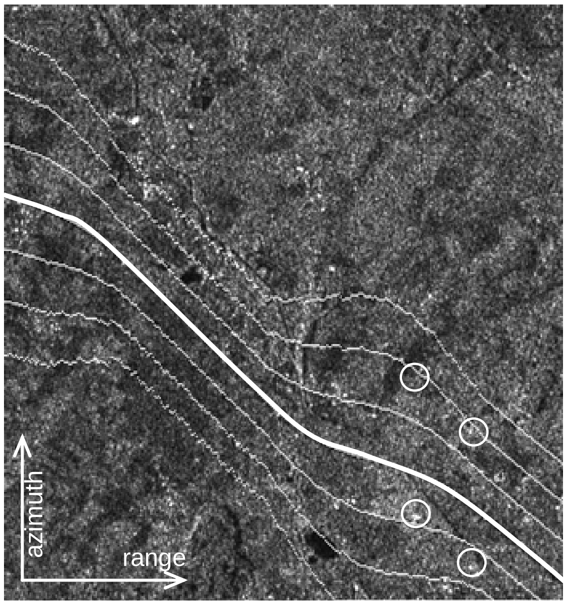

Figure 1 : SRTM X-SAR scene of an autobahn with moving targets, processed with the operational stationary target SAR processor. The fat line follows the road, the thin lines show the iso-velocity contours for multiples of 50 km/h. Circles mark presumably moving targets and their PRF ambiguities.

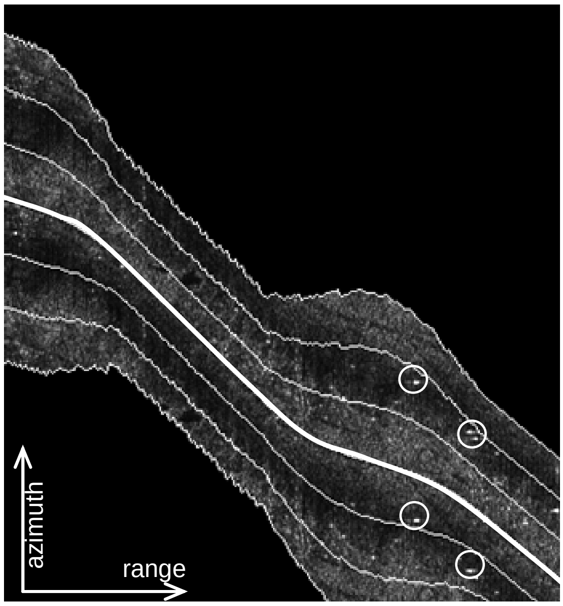

Figure 2 : SRTM X-SAR scene of an autobahn with moving targets processed with a time domain velocity adapted correlator. The possible signatures of moving objects and their PRF ambiguities are clearly visible. Also the clutter of the stationary area next the road is replicated in azimuth.